

# PROCEEDINGS OF SPIE

[SPIDigitalLibrary.org/conference-proceedings-of-spie](https://SPIDigitalLibrary.org/conference-proceedings-of-spie)

## Merging of imaging techniques based on reflectance hyperspectral and neutron tomography for characterization of a modern replica of a 13th century knife from Croatia

Francesco Grazzi, Costanza Cucci, Andrea Casini, Lorenzo Stefani, Nikolay Kardjilov, et al.

Francesco Grazzi, Costanza Cucci, Andrea Casini, Lorenzo Stefani, Nikolay Kardjilov, Adam Thiele, Jiří Hošek, Marcello Picollo, "Merging of imaging techniques based on reflectance hyperspectral and neutron tomography for characterization of a modern replica of a 13th century knife from Croatia," Proc. SPIE 11058, Optics for Arts, Architecture, and Archaeology VII, 1105816 (12 July 2019); doi: 10.1117/12.2526050

**SPIE.**

Event: SPIE Optical Metrology, 2019, Munich, Germany

# Merging of imaging techniques based on reflectance hyperspectral and neutron tomography for characterization of modern replicas of a 13th-century knife from Croatia

Francesco Grazzi<sup>a</sup>, Costanza Cucci<sup>a</sup>, Andrea Casini<sup>a</sup>, Lorenzo Stefani<sup>a</sup>, Nikolay Kardjilov<sup>b</sup>,  
Adam Thiele<sup>c</sup>, Jiří Hošek<sup>c</sup>, Marcello Picollo<sup>a</sup>

<sup>a</sup>Istituto di Fisica Applicata “Nello Carrara” - National Research Council (IFAC- CNR)

Via Madonna del Piano, 10 - 50019 Sesto Fiorentino (Florence) – Italy

<sup>b</sup>Helmholtz Zentrum Berlin – Hahn Meitner Platz, 1 – 14109 Berlin - Germany

<sup>c</sup>Archeologický ústav AV ČR, Praha, v. v. i. - Letenská 4 - 118 01 Praha 1 – Czech Republic

## ABSTRACT

A large amount of iron and steel artifacts produced in the central European area between 2nd and 14th Centuries is constituted by pattern welded iron-phosphoric iron and steel components. Phosphoric iron is a substitutional alloy, which is obtained by using iron ore from swamps in which decomposition of dead organisms enriches the iron rich soil with phosphorous. The identification of phosphoric iron alloy in ancient artifacts is important for determining their place of origin, production procedure and technological characteristics.

A well-established technique for investigating the bulk structure of ancient metallographic artifacts is neutron tomography, using cold neutrons. It provides image-data capable of enhancing differences between phosphorous rich iron and the standard iron areas. However, neutron imaging is costly and complex to implement. Therefore, the exploration of new techniques capable of providing additional data on the nature of alloys would be highly needed. A pilot study addressed to test the applicability of reflectance hyperspectral imaging to the investigation of ancient metallographic artifacts is presented here. So far this technique has been used for diagnostics of polychrome surfaces, but it has never been applied to investigation of metallic surfaces.

Hyperspectral imaging in the VIS-NIR range (400-1700 nm) was applied on replicas of a historical object from the archaeological site of Kobilic (Croatia). The same replicas were analyzed also using neutron tomography. Hyperspectral data were elaborated to map the distribution of the different phases on the surface. The comparison of the hyperspectral data with the neutron tomography data-images provided prominent similarities. These preliminary results encourage further investigations on merging these two imaging techniques for novel applications on archeo-metallurgy.

**Keywords:** Phosphoric iron, Neutron tomography, VIS-NIR Hyperspectral imaging, Non destructive analysis

## 1. INTRODUCTION

A large amount of iron and steel artefacts produced in Europe between the 2nd and 14th centuries AD were constituted from pattern-welded composites made of phosphoric-iron and steel components<sup>1</sup>. Phosphoric iron is a substitutional alloy in which a small amount of phosphorous is located into the ferrite lattice structure<sup>2-3</sup>. It is obtained by using iron ore from swamps in which decomposition of dead organisms enriches the iron rich soil with phosphorous<sup>4</sup>. This is a typical condition of large plains of Central Europe. This alloy provides no impressive improvements in mechanical performances of iron (a little increase in hardness and decrease in workability). Phosphoric iron has instead a much better resistance to oxidation and corrosion in general, thus improving the general stability of the whole artefact<sup>5</sup>. On the surface of the object, it can be optically distinguished from non-phosphor components because of its colour.

Identification of phosphoric iron in archaeological iron artefacts is important for determining the manner of their production and technological characteristics<sup>6</sup>.

At present, successful identification of phosphoric iron can be achieved by metallography (use of specific etchants such as Oberhoffer reagent) and measuring hardness of the metal matrix, or by determining the elemental composition of the metal<sup>7</sup>. As obvious, both these methods are invasive.

Another possible technique, less commonly used to characterize the bulk structure of metal ancient artefacts, is neutron tomography using cold neutrons<sup>8-9</sup>. In this class of artefacts, it provides image-data enhancing differences between the phosphorous rich iron areas and those containing standard iron and steel, into the object. Although neutron imaging is an effective and well-established method for the investigation of metallic artefacts, it is complex to implement because of the high costs and the limited accessibility to the few beam-line facilities available. Moreover, transport of important archaeological artifacts to the neutron facilities could constitute an issue. Therefore, the exploration of new techniques capable of providing additional data on the nature of alloys would be highly desired. In particular, taking into account that phosphoric iron is less prone to oxidation with respect to pure iron, imaging spectroscopy in the Visible (Vis) and Near Infrared (NIR) range appeared as a promising methodology to provide preliminary and fast indications about the nature of iron alloys in ancient artefacts.

So far, hyperspectral imaging has been successfully used for the non-invasive diagnostics of polychrome surfaces in several types of artworks, but it has never applied to investigate corroded metallic surfaces<sup>10</sup>.

In this work, a pilot study addressed to test the applicability of reflectance hyperspectral imaging to the investigation of ancient metallographic artefacts is presented. More specifically, the research aimed at exploring the complementarity between the 3D information provided by neutron tomography, and the 2D information provided by hyperspectral imaging applied to the investigation of ancient metallic artefacts produced using phosphoric iron. Thus, two modern replicas of an historical artefact from the archaeological site of Kobilic (Croatia) were analyzed using both neutron tomography and Vis-NIR hyperspectral imaging. The comparison of the reflectance hyperspectral data with the near surface neutron tomographic slice provided prominent similarities and evidenced the potential complementarity of the two imaging techniques for detecting and mapping the phosphorous content in metallic archeological artefacts.

These preliminary results encourage further investigations on merging these two imaging techniques belonging to diverse applicative areas. The next phase of this research will be the application of the technique to historical artefacts.

## 2. MATERIALS AND METHODS

### 2.1 Samples

Two modern replicas of ancient artefacts produced using the technique of pattern welding by combining multiple layers of iron and phosphoric iron were analyzed. The replicas were created in the framework of a PhD project of one of the co-authors (AT), who worked in trying to replicate the production steps of a phosphoric iron pattern welded knife retrieved in the archaeological site of Kobilic<sup>11</sup>. A preliminary study based on metallographic analysis on the original historical artefact was performed aimed at determining the relative composition, microstructure and pattern welding and shaping procedures applied to the production of this ancient knife. Based on the results obtained, several replicas were produced to formulate plausible hypothesis about the intermediate steps of the manufacturing process. An experimental archaeometallurgy program was therefore performed starting refining the phosphorous rich iron ore and preparing iron and phosphoric iron billets, which were then combined together according to a specific pattern welding procedure.

In the present study two replicas were analyzed:

- a) A billet corresponding to an intermediate working step in which all the future components of the finished knife are already assembled together (iron tang, pattern welded body with phosphoric iron layers, low carbon steel edge) even though not yet shaped.
- b) The finished knife in which all the aforementioned components are shaped and the phosphoric rich layers in the pattern-welded volume are clearly visible in areas on the two faces of the blade.

### 2.2 Instrumentation and experimental set-up

#### 2.2.1 Neutron imaging

Neutron imaging measurements were performed at the BER-II nuclear reactor of the Helmholtz Zentrum Berlin using the CONRAD-II beam-line<sup>12</sup>. This beam-line is a dedicated neutron imaging beam-line with neutron energy spectrum in the range of cold neutrons. This means that it provides the highest possible level of contrast between materials with close

composition and structure as pure ferrite and ferritic phosphoric iron. Both neutron absorption and scattering cross sections are modified by the presence of phosphorous<sup>13</sup>.

Tomography was performed using the following experimental parameters: L/D=400; Scintillator screen: Ag doped LiF/ZnS 200  $\mu\text{m}$  thickness; Field of view: 100x100 mm<sup>2</sup>; Acquisition time: 30 s; Sample – scintillator distance: 35 mm; number of projections: 400. Since a CCD 2048x2048 pixels was used, the digital spatial resolution was 49  $\mu\text{m}$  while, according to the experimental parameters (L/D, sample-scintillator distance, scintillator thickness) the image experimental spatial resolution turned out to be around 130  $\mu\text{m}$ .

The obtained projections for both samples were normalized by dark field subtraction and flat field ratio. Data treatment and tomography reconstruction were performed by using imageJ and Octopus codes<sup>14-15</sup>.

### 2.2.2 Hyperspectral imaging

Reflectance hyperspectral data were acquired using the latest version of the push-broom hyperspectral scanner designed at the IFAC-CNR laboratories, and recently readapted for investigating small sized objects featuring very fine details, typical sizes less than 1 mm<sup>16-17</sup>. In the present version, the hyperspectral scanner includes two spectrographic heads which operate in the [400-900] nm and [900-1650] nm ranges, respectively, thus covering the extended Visible (Vis) and the Near-Infrared (NIR) regions. The Vis spectrographic head includes a line spectrograph (Specim® ImSpector™ V10E) connected to a high-sensitivity Si CCD 1344x1024 pixels detector (mod. ORCA-ERG Hamamatsu®) and coupled with a telecentric objective (Opto-Engineering TL series). The NIR spectrographic head consists of a line spectrograph (Specim® ImSpector N17E) connected to an InGaAs 640x512 pixels detector (Xenics® mod. Xeva 1.7-640), and coupled with a NIR transmitting telecentric objective (Opto-Engineering TL series). The illumination system includes a 3200 K 150-Watt QTH-lamp connected to two fiber-optic illuminators, which symmetrically project their beams at 45° angles with respect to the normal direction at the imaged surface, thus providing a 2x45°/0° illumination/observation geometry. The 2x45°/0° configuration is prerequisite to extract calibrated RGB images and colorimetric values according to the CIE (Commission Internationale de l'Éclairage) recommendations for reflectance measurements for colorimetric applications<sup>18</sup>.

The spectrographic head and the illumination systems are fixed together on a mechanical structure, consisting of two high precision movements along orthogonal axes on a vertical-plane parallel to the painting surface.

The data acquisition is performed by scanning the target surface in free-run mode at a constant movement speed. In the present configuration the spatial sampling rate is 27 points /mm in the Visible range, and 9.2 points per mm in the NIR range. Based on preliminary laboratory tests, the overall spatial resolution of the system is 5 lines/mm in the Vis range and 2 lines/mm in the NIR range. The white reference calibration is performed by using a certified white reference Spectralon® 99% diffuse reflectance acquired before each measurements session.

### 2.2.3 Methodology

Phosphoric iron follows a different oxidation process with respect to pure iron, and it was hypothesized hyperspectral imaging might be able to reveal such differences in the spectrum.

Hyperspectral imaging measurements in the VIS-NIR range (400-1700 nm) were performed on the surface of the pattern welded phosphoric iron of the modern replicas which were also analyzed using neutron tomography, so that the phosphorous rich areas could be univocally identified throughout the entire object by using the latter method. The final aim of hyperspectral data processing was to provide a map of the distribution of the different mineralization phases on the surface and, due to the low chemical reactivity of phosphoric iron, discriminate the areas rich in phosphorous from the others.

Regarding the neutron tomography, it is known that neutron attenuation induced by phosphoric iron is as well lower than pure iron so that, in the neutron image data, such volumes appear darker than the ones made of pure iron.

A comparative investigation of hyperspectral elaborated images and neutron imaging data was performed, with the aim of identifying the spectral features that potentially can be used to discriminate phosphoric rich areas from pure iron areas in the examined artefacts.

### 3. RESULTS AND DISCUSSION

#### 3.1 Neutron imaging results

The neutron tomography data of the sample core clearly evidenced the presence of two distinct grey level volumes, which could be immediately ascribed to the ferrite / low carbon steel and to the phosphoric iron components.

Neutron images also evidenced that the welding procedure was performed in a very accurate way with no (or tiny) use of modern flux materials as borax. Indeed, boron is a highly absorbing element and it would have resulted in a bright area in tomography data, which is, instead, absent in our samples.

In the neutron image data, the dark grey volume is made of phosphoric iron while the light grey one is ferrite. It can be observed that the phosphoric iron is present in the pattern-welded volume of the billet (Figure 1) and in the small insert close to the back in the knife (Figure 2). The very fine and complex structure of the P-rich and pure Fe layers is clearly defined by the tomography results reported in Figures 1 and 2, where three different vertical tomography slices in the billet and the knife, respectively, are also reported.

In figures 1 and 2, the images with red and blue contour for both billet and knife are the closest images corresponding to the surface of the samples, so that they can be directly compared with the hyperspectral elaborated maps and with the visual inspection of the samples.

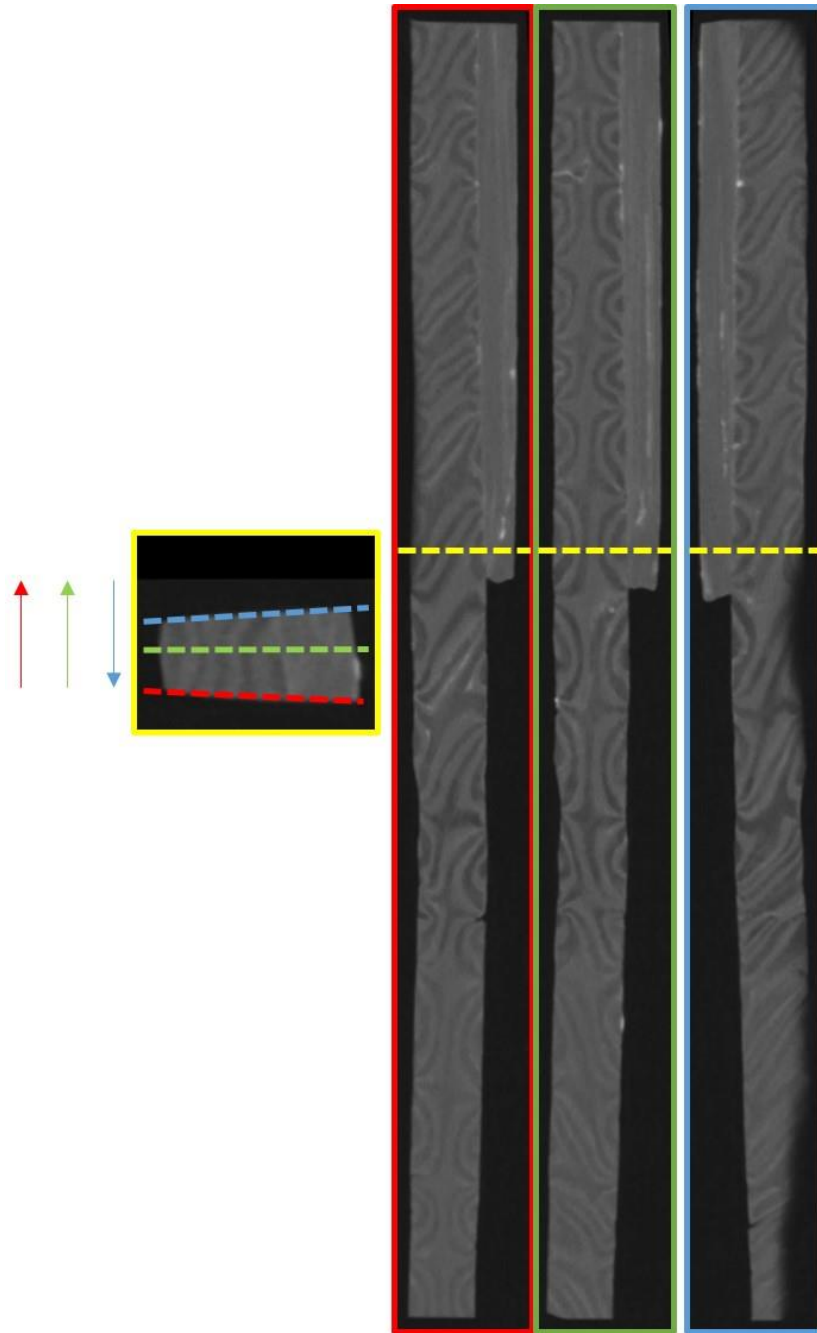


**Figure 1.** Tomography slices of the billet replica. The colour contour and dashed lines indicate the respective location of the sections. The three coloured arrows indicate the direction of view of the vertical sections in the horizontal slice. It is evident the variation of the pattern welding structure within the sample volume and the strong contrast between P-rich volume and the rest.

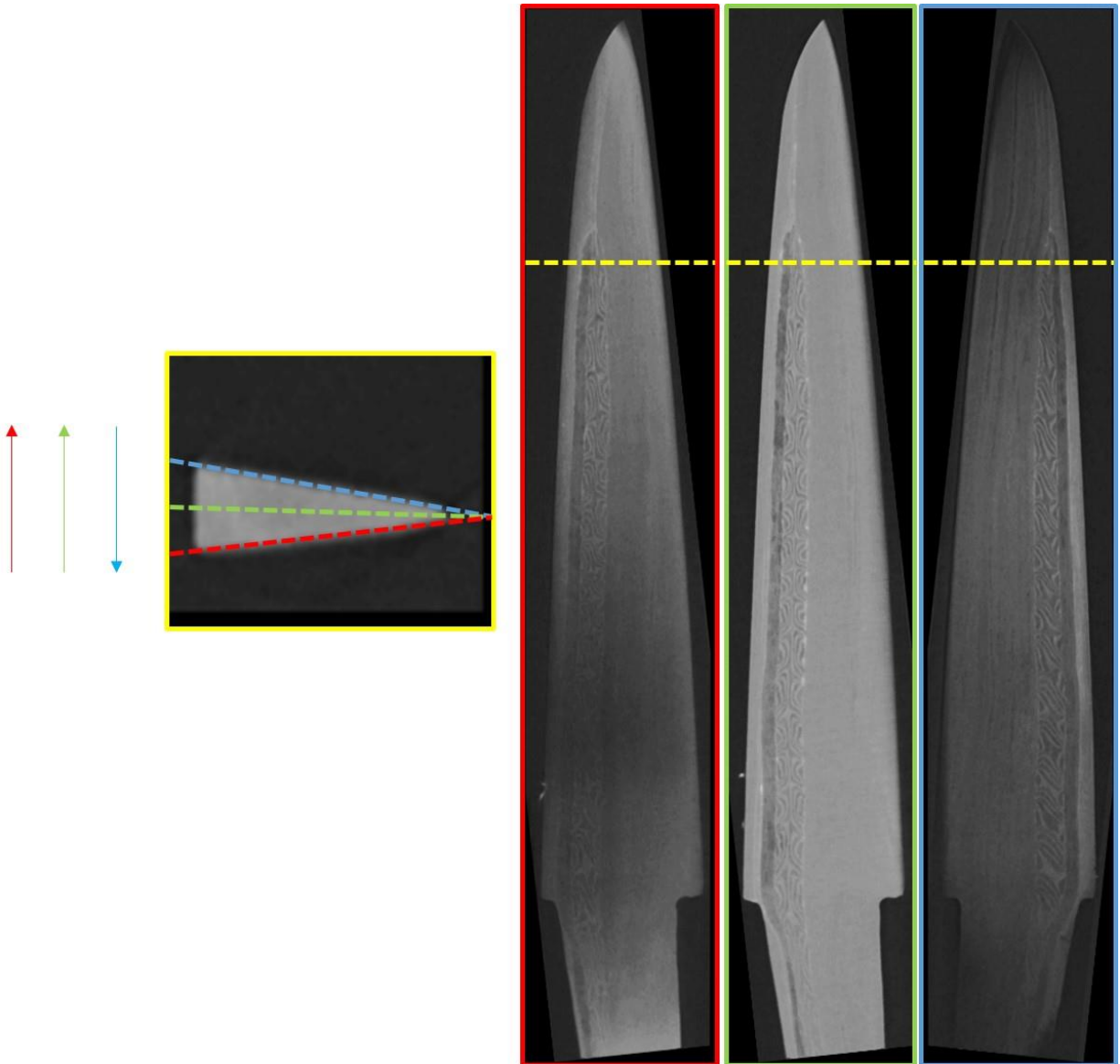


**Figure 2.** Tomography slices of the knife replica. The colour contour and dashed lines indicate the respective location of the sections. The three coloured arrows indicate the direction of view of the vertical sections in the horizontal slice. It is evident the variation of the pattern welding structure within the sample volume and the strong contrast between P-rich volume and the rest.

### 3.2 Hyperspectral imaging results

#### 3.2.1 Data processing

The acquisition of hyperspectral data on the knife replicas was a challenging task, due to some factors - such as the three-dimensional shape, the darkness and the shininess of the metallic surface - which made difficult the operative conditions for reflectance hyperspectral imaging measurements. Indeed, ideally the surface to be imaged should be almost flat, placed on a vertical plane at a fixed distance from the optical lens of the objective, so as to ensure the best conditions for a uniform illumination and also for an optimal focalization distance. Due to the 3D shape of the examined objects, optimal focus could be achieved only on a selected area of the object surface, with unavoidable blurring effects on the other parts. Moreover, since metallic surfaces are inherently shining, the illumination/collection geometry was a critical issue. Indeed,

the irregular shape and the presence of multiple edges and acute angles caused undesired reflections resulting in undesired local saturations in the output image. Moreover, the darkness of the surface of the examined objects, which appears as almost black at the visual inspection, unavoidably encompassed a reduction of the intensity of reflectance signal.

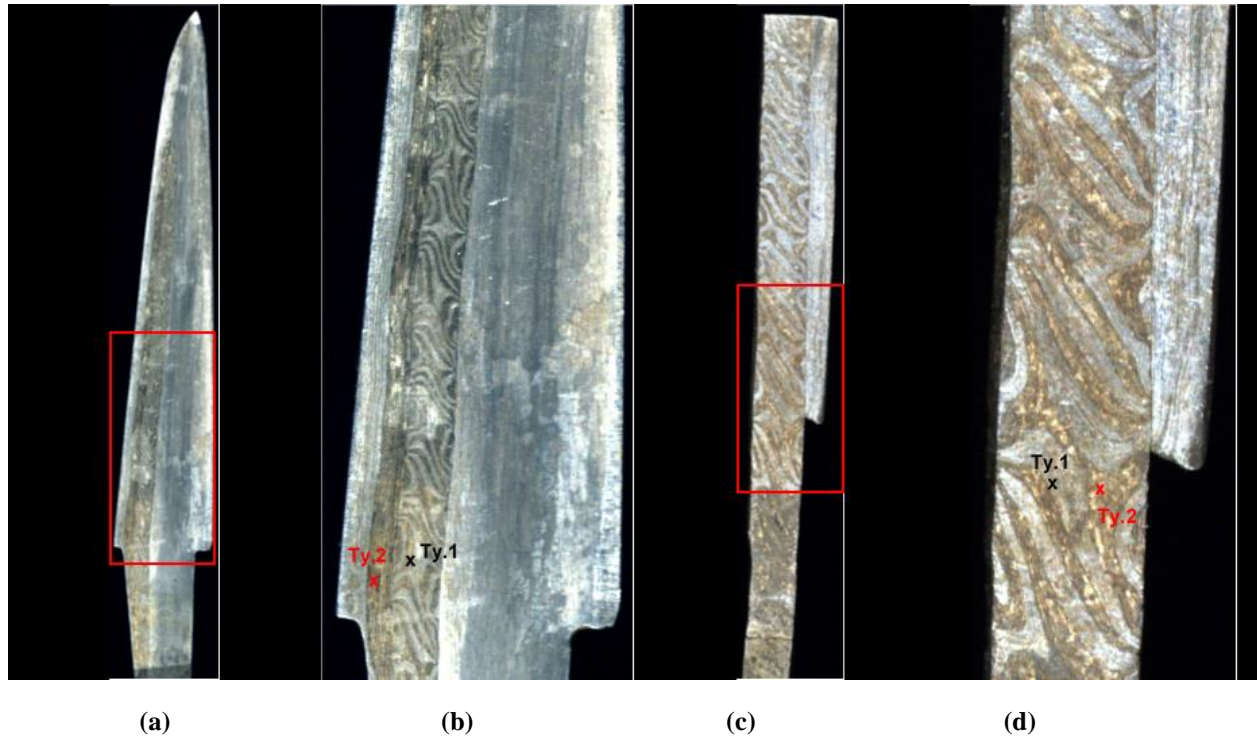


**Figure 3** - High resolution RGB colour calibrated images obtained by the Vis reflectance hyperspectral data. The two iron phases are indicated as Type 1 and Type 2, and are distinguishable based on their different colours. a) The knife; b) Detail of the pattern welded insert with the positions of extraction of Vis spectra; c) The billet; d) Detail the pattern welded volume with the positions of extraction of Vis spectra.

The aforementioned factors were sources of spectral noise, which degraded the quality of reflectance data. Therefore, the data-cubes acquired in the 400-900 nm range and 900-1650 nm range were preliminarily, and separately, pre-processed, using different denoising algorithms. Inverse Maximum Noise Fraction (MNF) method was used for the NIR data-cube, whereas spatial average was applied to the Vis data-cube, in order to smooth the reflectance spectra<sup>19</sup>.

Data-processing of hyperspectral data cubes was performed using ENVI® software.

### 3.2.2 Vis 400-900nm data

At first, the hyperspectral data acquired in the 400-900 nm range were used to reconstruct a high definition RGB image of the surface, reported in Figure 3. Thanks to the high spatial sampling rate of the system, the extracted color image features high spatial definition, enabling visualization of the finest details, along with the imperfections and irregularities of the surface. In Figure 3, the hand-crafted patterns created by alternation of phosphoric and pure iron are clearly recognizable. It can be noticed that the RGB images are fully consistent with those obtained by neutron imaging technique. In addition, since the calibrated RGB images were reconstructed from the hyperspectral data-cube, they include a spectral information associated to each pixel. Therefore, it is possible to visualize the spectra associated to the different coloured areas from any desired point of the reconstructed image. A drawback of high spatial sampling is that, due to the reduced size of the pixel, each spectrum is averaged over a smaller area. This encompasses a very low signal-to-noise ratio and, hence, the choice of suitable smoothing algorithms. After several trials with different smoothing algorithms, the best option for the present data-set resulted to be spatial resizing, based on an average over a selected number of adjacent pixels. Using this

approach, the average spectra of the two iron components, corresponding to differently colored areas in the RGB image, were extracted in correspondence of points reported in Figures 3b and 3c, for the two samples.

The comparative analysis with the neutron images indicated that the iron-phase named as “Type 1” in Figures 3b and c, appearing as light grey in the RGB color image, corresponds to the lighter areas in the neutron images, and should be therefore associated to pure iron. Instead, the iron phase classified as “Type 2” in Figures 3b and c, featuring a reddish-yellow color in the RGB image, corresponds to the darker areas in the neutron image, and can be likely associated to phosphoric iron.

Figure 4 shows the average spectra of “Type 1” and “Type 2” iron components. It can be observed that different spectral behaviors are associated to the two iron-phases, essentially due to a slightly different trend in the 450-500nm region. However, although clearly distinguishable, the two iron components do not feature in the Vis region a clear spectral signature attributable to the different chemical contents.

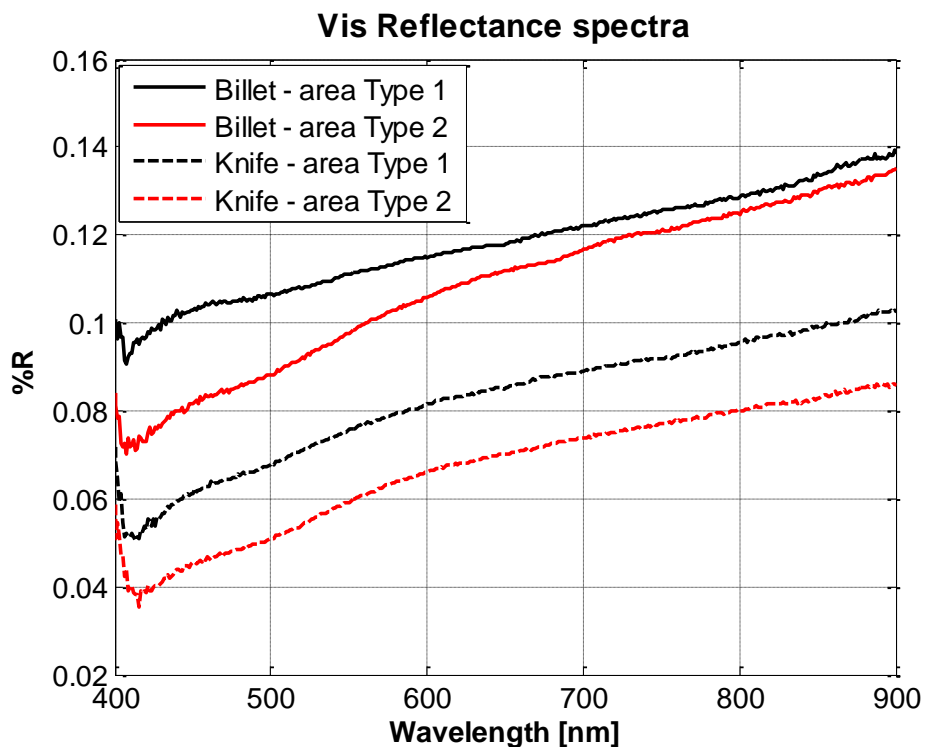


**Figure 4.** Average spectra of the two different iron phases (Type 1 and Type 2) extracted from the Vis data-cube in correspondence of the positions indicated in Figures 3b and 3d for the billet and the knife

### 3.2.3 NIR 900-1650 nm data

Due to the lower spatial sampling of the NIR spectrographic head, the quality of images acquired in the NIR is poorer than in the Vis. Conversely, the signal-to-noise ratio of the spectral data in the 900-1650 nm range is much better than in the Vis. This circumstance made it possible to apply smoothing algorithms that could not be used to treat the Vis data. The NIR data-cube was pre-processed by using firstly the MNF compression algorithm, and subsequently the inverse MNF transformation in order to obtain a set of smoothed spectra.

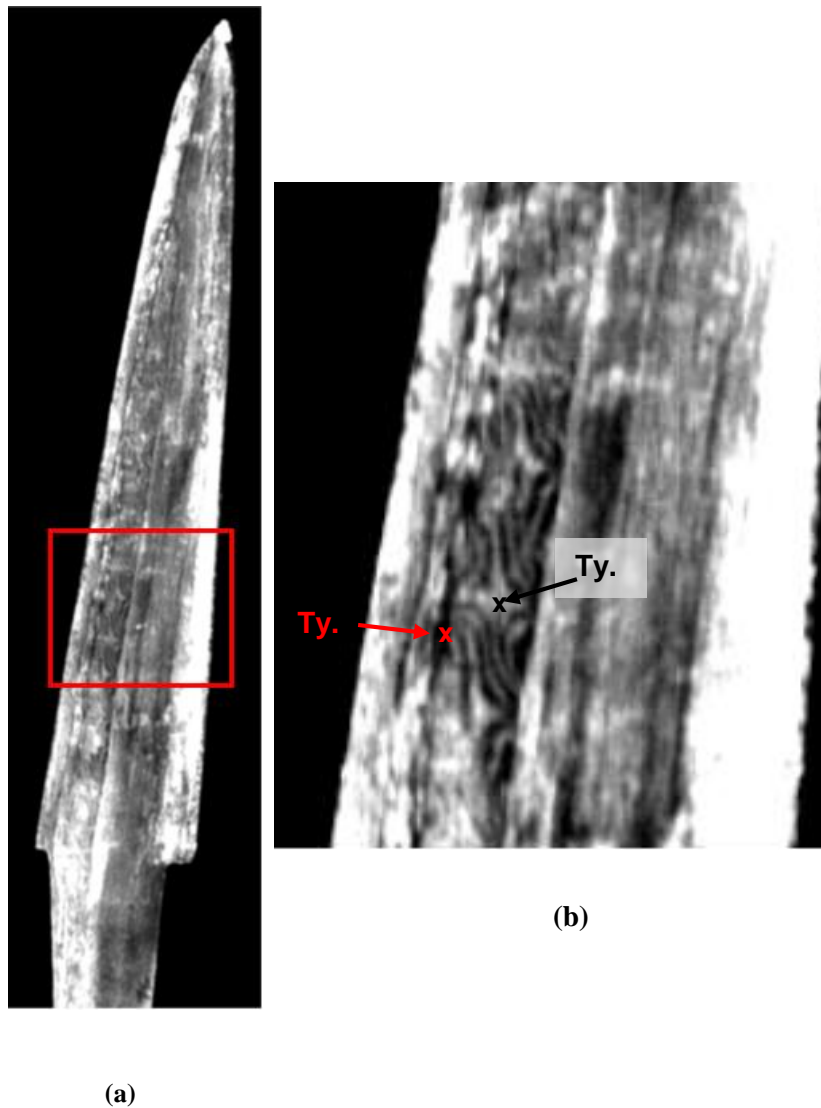


**Figure 5** a) Spectral image of the knife at 1334nm. b) Detail of the pattern welded insert with the positions of extraction of NIR spectra

Figure 5 shows the spectral image extracted from the data-cube at 1334 nm. At this wavelength, the best image contrast could be obtained, thanks to the combination of maximum in reflectance of the target surface, along with the maximum in the sensitivity curve of the NIR sensor. Since the focalization was not optimal all over the imaged scene because of the three-dimensionality of the object, some undesired local saturation effects are observable in the output image (Figure 5a). However, in the central area of the image (Figure 5b), it is still possible to recognize the typical welded patterns created by the different layers of phosphoric and pure iron. The comparison of the 1334 nm image with the reconstructed RGB image (Fig 3b) lead to classify the darker areas as “Type 2” (phosphoric-iron), and the clearer areas as “Type 1” (pure iron). Hence, reflectance spectra were extracted from the NIR data-cube at the points indicated in Figure 5b, that is in correspondence of dark and clear areas. The curves are reported in Figure 6. It can be observed that the two iron components are distinguishable for the presence of the absorption band around 1250 nm, which

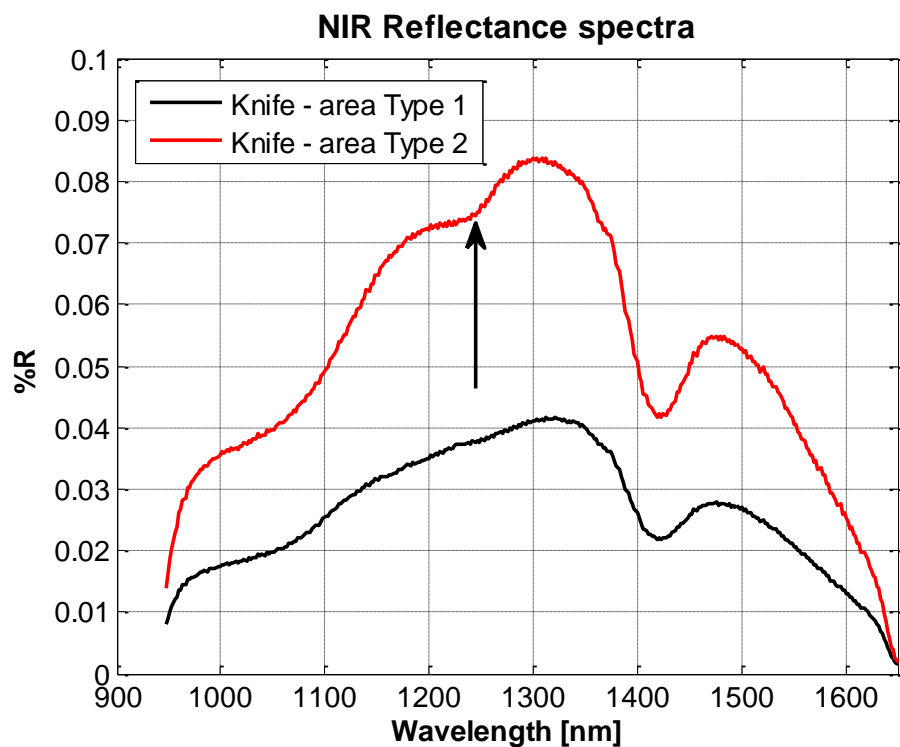


**Figure 6.** The reflectance spectra of the two different iron phases (Type 1 and Type 2) extracted from the NIR data-cube for the knife at the positions indicated in Figure 5b.

appears in the reflectance spectrum of “Type 2” component. This would suggest that this spectral feature could be related to the presence of phosphoric-iron. Based on this guess, the spectral image selected at 1250 nm was used to elaborate a map with enhanced contrast, reported in Figure 7a. It can be observed that the welded patterns are much more evident in this image, and are fully consistent with the neutron image extracted at the surface of the knife (Figure 7b). This result corroborates the hypothesis of the correlation between the spectral band at 1250 nm and the presence of phosphoric iron.



**Figure 7.** a) Elaborated map of the knife obtained from the 1250nm spectral image acquired with hyperspectral imaging technique. b) Neutron image tomography, extracted at the surface of the knife.

## 4. CONCLUSIONS

A pilot study addressed to explore the complementarity between neutron tomography and reflectance hyperspectral imaging techniques for the investigation of ancient metallic artefacts is presented. To this aim, two modern replicas produced using the same manufacturing technology of a 13th Century knife, retrieved in the archaeological site of Kobilić (Croatia) were analyzed using both the 3D and 2D imaging techniques. The acquired experimental data demonstrated that both neutron imaging and reflectance hyperspectral imaging are capable of discriminating the presence of phosphoric iron in the examined artefacts, providing a distribution map of the material over the surface (hyperspectral imaging) or into the volume (neutron tomography) of the object.

Neutron tomography data clearly evidenced the presence of phosphoric iron volumes and demonstrated to be a useful method for 3D reconstruction of P-rich iron distribution within historical samples. Mineralization effects could affect the level of contrast among the various components so that another test experiment to be performed on historical phosphoric iron artefacts is desired before definitely stating the method.

The hyperspectral imaging results showed that the colorimetric features, as well as typical spectral signatures in the NIR range can be correlated to the presence of phosphoric iron, thus providing a promising tool to map the presence of this material and discriminate it from different components, such as pure iron.

Despite the very preliminary stage of this research, the results obtained appeared highly promising and encourage further investigations. The next phase of this research will be aimed at deepening the interpretation of the NIR spectroscopic data, as well as extending the methodology to the study of original historical artefacts

## ACKNOWLEDGEMENTS

We thank HZB for the allocation of neutron radiation beamtime.

## REFERENCES

- [1] Buchwald, V. F., [Iron and steel in ancient times], Det Kongelige Danske Videnskabernes Selskab, Copenhagen, 2005.
- [2] ASM International, [ASM Handbook Vol. 3, Alloy Phase Diagrams], ASM International, 1992.
- [3] Pearson, W. B., [A Handbook of Lattice Spacings and Structures of Metals and Alloys], Pergamon Press, 1958.
- [4] Smith, C. S., [A Search for Structure], MIT Press, 1981.
- [5] Craddock, P. T., [Early Metal Mining and Production], Smithsonian Institution Press, 1995.
- [6] Stewart, J.W., Charles, J.A., Wallach, E.R. "Iron–phosphorus–carbon system: Part 3 – Metallography of low carbon iron–phosphorus alloys." *Materials Science and Technology* 16(3), 291-303 (2000).
- [7] Thiele, A. and Hošek, J., "Estimation of Phosphorus Content in Archaeological Iron Objects by Means of Optical Metallography and Hardness Measurements" *Acta Polytechnica Hungarica* 12(4), 113 (2015)
- [8] Grazzi, F., Salvemini, F., Kaestner, A., Civita, F., Lehmann, E. H. and Zoppi, M., "Characterization of two Japanese ancient swords through neutron imaging" *Hamon* 25(3), 206-213 (2015).
- [9] Grazzi, F., Cantini, F., Salvemini, F., Scherillo, A., Schillinger, B., Kaestner, A., Edge, D. and Williams, A., "The investigation of Indian and central Asian swords through neutron methods" *J. Arch. Sci. Rep.* 20, 834-842 (2018).
- [10] Cucci, C., Delaney, J. K., Picollo, M. "Reflectance hyperspectral imaging for investigation of works of art: old master paintings and illuminated manuscripts." *Accounts of chemical research* 49(10), 2070-2079 (2016).
- [11] Thiele, A. "The manufacturing technology of a pattern-welded knife from Kobilić (Republic of Croatia)." *Archeologické Rozhledy* LXX, 457-467 (2018).
- [12] Kardjilov, N., Hilger, A., Manke, I., Strobl, M., Dawson, M., Williams, S. and Banhart, J., "Neutron tomography instrument CONRAD at HZB" *Nucl. Instr. and Meth. in Phys. Res. A* 651, 47-52 (2011).

- [13] <https://www.nist.gov/ncnr/planning-your-experiment/sld-periodic-table>
- [14] Schneider, C. A., Rasband, W. S. and Eliceiri, K. W., "NIH Image to ImageJ: 25 years of image analysis" *Nature methods* 9(7), 671-675 (2012).
- [15] Dierick, M., Masschaele, B. and van Hoorebeke, L. "Octopus, a Fast and User-friendly Tomographic Reconstruction Package Developed in LabView®" *Meas. Sci. Technol.* 15, 1366-1370 (2004).
- [16] Cucci, C., Casini, A., Picollo, M., Stefani, L., Pezzati, L., "Extending hyperspectral imaging from VIS to NIR spectral regions: a novel scanner for in-depth analysis of polychrome surfaces" *Proc. SPIE 8790 Optics for Arts, Architecture, and Archaeology IV*, 8790091-8790099 (2013).
- [17] Cucci, C., Casini, A., Picollo, M., Poggese, M., Stefani, L., "Open issues in hyperspectral imaging for diagnostics on paintings: when high spectral and spatial resolution turns into data redundancy", *Proc. SPIE 8084 O3A: Optics for Arts, Architecture, and Archaeology III*, 80848.1-80848.10 (2011).
- [18] CIE 15:2004 Technical Report, *Colorimetry 3rd edn.* (Commission Internationale de l'Eclairage (CIE), Central Bureau of the CIE, Vienna). ISBN 3 901 906 33 9.
- [19] Green, A.A., Berman, M., Switzer, P. and Craig, M.D., "A transformation for ordering multispectral data in terms of image quality with implications for noise removal". *IEEE Transactions on geoscience and remote sensing*, 26(1),.65-74 (1988).